Chin. J. Astron. Astrophys. Vol. 3 (2003), No. 3, 241–246
(http://www.chjaa.org or http://chjaa.bao.ac.cn)

Chinese Journal of Astronomy and Astrophysics

Coronal Flux Rope Equilibria in Closed Magnetic Fields *

Zhen Wang and You-Qiu Hu

School of Earth and Space Sciences, University of Science and Technology of China, Hefei 230026; huyq@ustc.edu.cn

Received 2002 June 10; accepted 2003 March 26

Abstract Using a 2.5-dimensional ideal MHD model in Cartesian coordinates, we investigate the equilibrium properties of coronal magnetic flux ropes in background magnetic fields that are completely closed. The background fields are produced by a dipole, a quadrupole, and an octapole, respectively, located below the photosphere at the same depth. A magnetic flux rope is then launched from below the photosphere, and its magnetic properties, i.e., the annular magnetic flux Φ_p and the axial magnetic flux Φ_z, are controlled by a single emergence parameter. The whole system eventually evolves into equilibrium, and the resultant flux rope is characterized by three geometrical parameters: the height of the rope axis, the half-width of the rope, and the length of the vertical current sheet below the rope. It is found that the geometrical parameters increase monotonically and continuously with increasing Φ_p and Φ_z: no catastrophe occurs. Moreover, there exists a steep segment in the profiles of the geometrical parameters versus either Φ_p or Φ_z, and the faster the background field decays with height, the larger both the gradient and the growth amplitude within the steep segment will be.

Key words: Sun: magnetic fields — Sun: corona

1 INTRODUCTION

Coronal magnetic flux ropes are typical structures in the solar corona that are simple enough to be tractable. They may coexist with prominences whose magnetic field is opposite to the photospheric polarity beneath them (Low & Hundhausen 1995). Many studies have been carried out in terms of 2-D approximations to find magnetostatic equilibrium solutions that involve a levitating flux rope embedded in a bipolar background field. The focus is on whether there exists a catastrophe for the system that is aimed at elucidating various solar explosive phenomena (Forbes & Isenberg 1991; Forbes & Priest 1995; Isenberg et al. 1993; Lin et al. 1998, 2001; Hu & Liu 2000; Hu 2001; Hu et al. 2001; Hu & Jiang 2001; Li & Hu 2001). If a catastrophe occurs, a current sheet will be formed and extended at the Alfvén timescale below the erupting flux rope. This will in turn provide a favorable condition for a rapid magnetic

* Supported by the National Natural Science Foundation of China.

reconnection, leading to a sudden release of magnetic energy. A common conclusion of these studies is that catastrophe exists under certain conditions. However, if the background field is completely closed, the radius of the cross section of the flux rope must be less than a certain critical value in order that a catastrophe may occur (Forbes & Priest 1995). Namely, for flux ropes of large cross section, no catastrophe exists for the system, and this conclusion was further confirmed by Hu & Liu (2000, referred to as Paper I hereinafter). On the other hand, if the background field is partly opened, catastrophe becomes a general phenomena in solar active regions (Hu 2001; Hu & Jiang 2001).

In Paper I, the background magnetic field is produced by two uniform surface charges of opposite polarity at the photosphere. No catastrophe occurs for the system in this case. One may naturally ask whether the same conclusion holds if a different type of closed field is taken to be the background, and if so, what the effect of the pattern of the background field is on the equilibrium properties of the related flux rope. We will answer these questions in the present paper, taking three different background fields that are produced by a dipole, a quadrupole and an octapole located below the photosphere at the same depth.

2 BACKGROUND FIELDS AND EMERGENCE OF FLUX ROPE

Take a Cartesian coordinate system such that the photosphere coincides with the x-z plane and the y-axis is vertical and upward. For two-dimensional problems independent of z, one may introduce a magnetic flux function $\psi(t, x, y)$ related to the magnetic field by

$$\boldsymbol{B} = \nabla \times (\psi \hat{\mathrm{z}}) + B_z \hat{\mathrm{z}}\,. \tag{1}$$

We use time-dependent simulations to obtain new equilibrium solutions for magnetic configurations that consist of a levitating flux rope and a closed background field. The basic equations are the same as those used in Paper I or taken by Hu et al. (2001). The computational domain is taken to be $0 \le x \le 3$ and $0 \le y \le 24$ in units of $L_0 = 10^4$ km, and discretized into 60×120 uniform meshes. Relevant boundary conditions are the same as those taken in Paper I.

The initial corona is isothermal and static with $T = T_0 = 10^6$ K and $\rho = \rho_0 = 3.34 \times 10^{-13}$ kg m^{-3} at the base. The initial background magnetic fields are assumed to be potential and symmetrical relative to the y-axis. They are produced by a dipole, a quadrupole and an octapole, respectively, located at $x = 0$ and $y = -1$. Incidentally, while the dipole and quadrupole fields have 2 and 4 poles on the solar surface, respectively, the octapole field does not mean 8 poles on the solar surface, but actually, it has 6 poles at most, if the extent of interest along the x-direction is sufficiently large. These fields can be cast in the complex variable form

$$f(\omega) \equiv B_x - iB_y = \frac{1}{(\omega+i)^2}\,, \quad \frac{2i}{(\omega+i)^3}\,, \quad -\frac{3}{(\omega+i)^4}\,, \tag{2}$$

respectively, where $\omega = x + \mathrm{i}\,y$. The corresponding magnetic flux functions are then given by

$$\psi_i = \mathrm{Im}\left\{\int f(\omega)\mathrm{d}\,\omega\right\}\,, \tag{3}$$

and they are

$$\psi_i(x,y) = \frac{y+1}{x^2+(y+1)^2}\,, \quad \frac{(y+1)^2-x^2}{[x^2+(y+1)^2]^2}\,, \quad \frac{(y+1)^3-3(y+1)x^2}{[x^2+(y+1)^2]^3}\,, \tag{4}$$

for the dipole field, quadrupole field, and octapole field, respectively. All of these magnetic flux functions have been normalized to unity at the origin, and vanish at infinity. The magnetic field strength at the origin can be evaluated from Equation (2) by taking $\omega = 0$, and it reads 1 for the dipole field, 2 for the quadrupole field, and 3 for the octapole field. Figure 1 shows the magnetic configurations of these fields in terms of the contours of ψ, which are uniformly spaced 0.1 apart so that the field strength may be intuitively judged according to the density of these contours. As can be intuitively seen from Figure 1, for the dipole (octapole) field, the field is the weakest (strongest) at the origin, and decays most slowly (rapidly) with height. To be more quantitative, the field strength along the y-axis ($\omega = iy$) decays as fast as $(y+1)^{-2}$, $(y+1)^{-3}$, and $(y+1)^{-4}$, respectively. As a result, the dipole and the quadrupole fields at $y = 1$ and the octapole field at $y = 0.732$ have the same strength, while the quadrupole and octapole fields are equally strong at $y = 0.5$. As we move to higher altitudes, the dipole field eventually becomes the strongest and the octapole field, the weakest. Such distributions of the background field strength with height have a subtle influence on the equilibrium property of the system, as we will see later on.

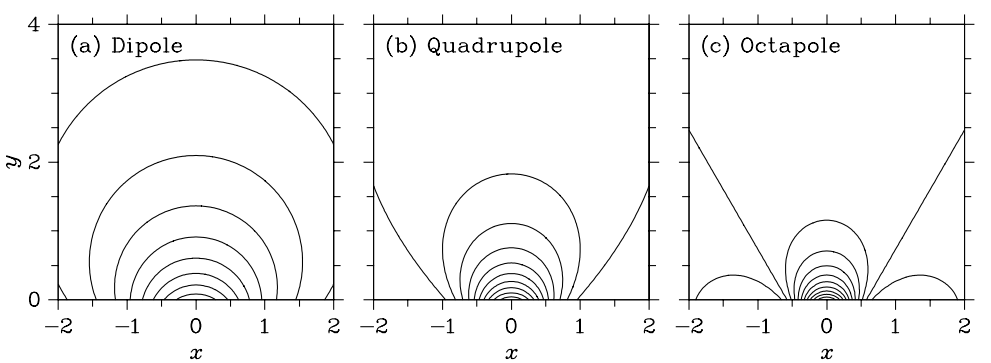

Fig. 1 Magnetic configurations created by (a) a dipole, (b) a quadrupole, and (c) an octapole, located at $x = 0$ and $y = -1$.

Following Paper I, we assume that a magnetic flux rope of circular cross section begins to emerge at $t = 0$ in the central area of the base, and becomes fully detached from the photosphere after $t = \tau_E$. The radius of the rope is a, and the emergence is uniform in velocity. The emerging part of the rope is bounded by $x = \pm x_E$ at time t, where

$$x_E = (a^2 - h_E^2)^{1/2}\,, \qquad h_E = a(2t/\tau_E - 1)\,. \tag{5}$$

At the base of the emerging part of the rope ($y = 0, |x| \le x_E$) the relevant quantities are specified as a function of t and x as follows:

$$\psi(t,x,0) = \psi_i(x,0) + \psi_E(t,x)\,, \tag{6}$$

$$\psi_E(t,x) = \frac{C_E}{2} \ln\left(\frac{2a^2}{a^2 + x^2 + h_E^2}\right)\,, \tag{7}$$

$$B_z(t,x,0) = C_E a (a^2 + x^2 + h_E^2)^{-1}\,, \tag{8}$$

$$v_y(t,x,0) = 2a/\tau_E\,, \qquad v_x(t,x,0) = v_z(t,x,0) = 0\,, \tag{9}$$

$$T(t,x,0) = 0.02\,, \qquad \rho(t,x,0) = 50\,, \tag{10}$$

where C_E is a constant and controls the magnetic properties of the emerging rope. At $t = 0.5\tau_E$, we have $h_E = 0$ and $x_E = a$ from Equation (5), implying that half of the flux rope has emerged from below the photosphere and the rope axis lies exactly at the origin. At this time, both ψ_E and B_z reach their maxima at the origin, which are $0.347C_E$ and C_E, respectively, derived from Equations (7) and (8) with $x = h_E = 0$. After $t = \tau_E$, the state at the base returns to the original. The 2.5-dimensional ideal MHD equations are solved by the multistep implicit scheme developed by Hu (1989) to find out equilibrium solutions of the whole system.

3 EQUILIBRIUM PROPERTY OF CORONAL FLUX ROPES

In the following numerical examples, we fix $a = 0.3$, $\tau_E = 5\ \tau_A$, and $\beta = 2\mu_0\rho_0 RT_0/B_0^2 = 0.1$. The numerical units of the other quantities are then $B_0 = (2\mu_0\rho_0 RT_0/\beta)^{1/2} = 3.73\ \times 10^{-4}$ T for the magnetic field strength, $\psi_0 = B_0 L_0 = 3.73\ \times 10^3$ Wb m^{-1} for the magnetic flux function, $\Phi_0 = B_0 L_0^2 = 3.73\ \times 10^{10}$ Wb for the magnetic flux, etc. The characteristic Alfvén speed is $v_A = B_0/(\mu_0\rho_0)^{1/2} = 575$ km s^{-1}, and the Alfvén transit time is $\tau_A = L_0/v_A = 17.4$ s. These values are the same as those in Paper I or in Hu et al. (2001). Calculations are made for different emergence parameter C_E and for each of the three background fields mentioned above. For each case, the system undergoes a temporal evolution and eventually reaches equilibrium. We then calculate the annular magnetic flux of unit length along the flux rope axis, Φ_p, which is simply the difference in ψ between the axis and the outer boundary of the rope, and the axial magnetic flux passing through the cross section of the flux rope, Φ_z. Also calculated are the following three geometrical parameters of the flux rope: the height of the rope axis, the half-width of the rope, and the length of the newly formed current sheet below the flux rope, denoted by h_a, w, and h_s, respectively hereinafter.

Numerical calculations show that both Φ_p and Φ_z increase monotonically and smoothly with increasing C_E, and their profiles depend on the pattern of the initial background field. In view of the fact that Φ_p and Φ_z are physically more meaningful than C_E, the geometrical parameters will be shown below as a function of either Φ_p or Φ_z instead of C_E. The reader should be reminded, however, that the two magnetic fluxes are not independent in the present case, but vary synchronously with the emergence parameter C_E.

Figure 2 shows the length of the current sheet h_s, the height of the rope axis h_a, and the half-width w as functions of Φ_p (Figs. 2a-2c) and Φ_z (Figs. 2d-2f) for the three background field cases, respectively. As seen from this figure, all the geometrical parameters vary monotonically and continuously with both Φ_p and Φ_z and no catastrophe occurs. This confirms the conclusion reached in Paper I that a system consisting of a levitating flux rope and a closed background field has no catastrophe. Nevertheless, certain differences exist between the three background field cases, implying that the pattern of the background field affects the equilibrium properties of the system. The main differences are summarized below.

1. From Figures 2a and 2d, the flux rope sticks to the photosphere when Φ_p and Φ_z are small. There exists a critical value of either Φ_p or Φ_z, at which the flux rope begins to leave the photosphere and the current sheet starts to appear. The critical values are $\Phi_p = 0.65$ and $\Phi_z = 1.30$ for the dipole case, 0.50 and 0.85 for the quadrupole case, and 0.33 and 0.46 for the octapole case. Namely, they are the highest for the dipole case and the lowest for the octapole case. This stems from the fact that the dipole has the largest field strength at higher altitudes so as to make the expanded flux rope most difficult to be separated from the photosphere.

2. Right after the flux rope starts to leave the photosphere, the profiles of h_s and h_a undergo a relatively steep variation with either Φ_p or Φ_z and then return to normal. Both the gradient and the growth amplitude in the steep variation region are the largest for the octapole case and smallest for the dipole case. The reason also lies in that the dipole has the largest field strength at high altitudes where the expanded flux rope is located. However, the profiles of w are similar in the three cases. This is because the field lines on the left and right sides of the levitating flux rope are stretched and nearly aligned along the vertical direction, so the background field strength is mainly determined by the total magnetic flux emanating from the photosphere, i.e., $\psi(0,0)$, which is unity for all three background fields. As a result, the transverse constraint provided by the background field turns out to be about the same for the three cases, leading to a nearly the same half-width of the flux rope.

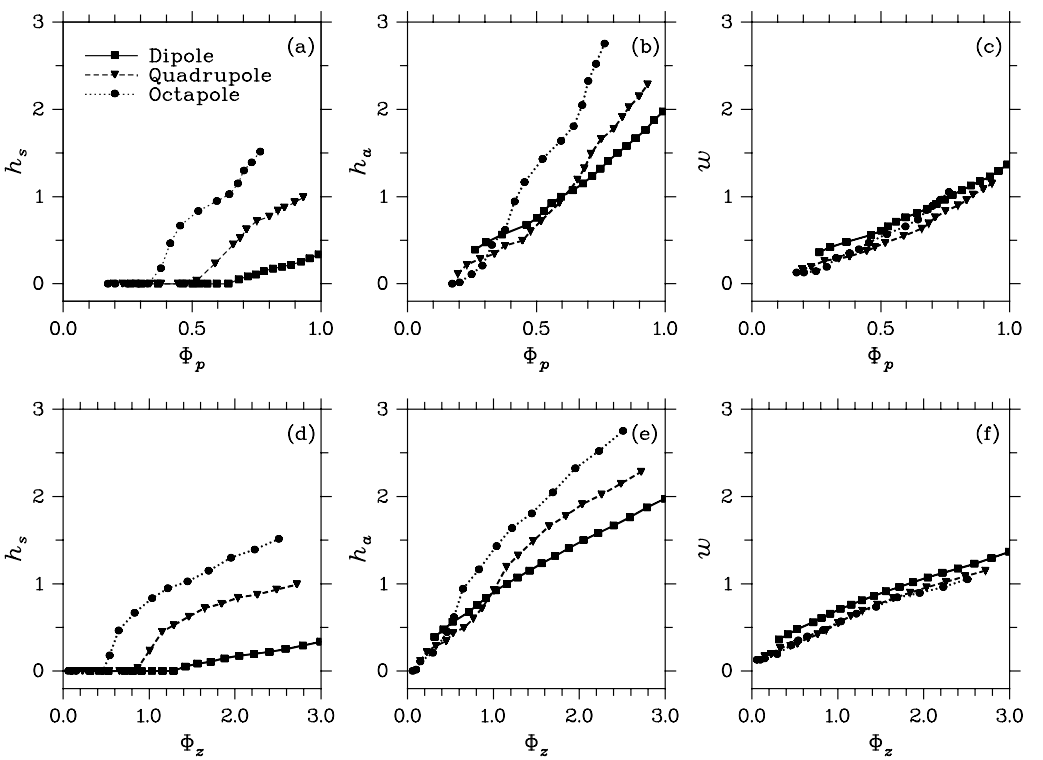

Fig. 2 Length of the current sheet h_s, height of the rope axis h_a, and half-width of the rope w versus the annular magnetic flux Φ_p (a-c) and axial magnetic flux Φ_z (d-f) of the flux rope for the three background field cases.

4 CONCLUDING REMARKS

Using a 2.5-D ideal MHD model, we conduct a numerical study of the equilibrium properties of coronal magnetic flux ropes embedded in closed background magnetic fields. Three types of background fields are tested, produced by a dipole, a quadrupole and an octapole, which are located below the photosphere at the same depth. It is found that no catastrophe exists for

such a system, a conclusion agreeing with that reached in Paper I for a closed background field created by two separate photospheric surface magnetic charges of opposite sign. The system undergoes a steep variation with either the annular magnetic flux or the axial magnetic flux of the flux rope after the rope starts to leave the photosphere. The gradient and the growth amplitude within the steep variation region depend on the variation of the background field with height: the faster the background field decays with height, the larger the gradient and the growth amplitude will be. If the decay of the background field is further quickened, the steep region might become narrower and the growth amplitude of the geometrical parameters of the flux rope might become larger, which is closer to the catastrophic case. However, based on the results obtained in the present paper, it is our belief that a veritable catastrophe would not exist for magnetic configurations that consist of a levitating flux rope and a fully-closed background field.

Acknowledgements This work was supported by grant NKBRSF G2000078404, grants NNSFC 40274049 and 10233050, and the Innovation Engineering Fund of the University of Science and Technology of China.

References

Forbes T. G., Isenberg P. A., 1991, ApJ, 373, 294
Forbes T. G., Priest E. R., 1995, ApJ, 446, 377
Hu Y. Q., 1989, J. Comput. Phys., 84, 441
Hu Y. Q., 2001, Solar Phys., 200, 115
Hu Y. Q., Jiang Y. W., 2001, Solar Phys., 203, 309
Hu Y. Q., Liu W., 2000, ApJ, 540, 1119 (Paper I)
Hu Y. Q., Jiang Y. W., Liu W., 2001, Chin. J. Astron. Astrophys., 1, 77
Isenberg P. A., Forbes T. G., Démoulin P., 1993, ApJ, 417, 368
Li G. Q., Hu Y. Q., 2001, Chinese Science (Series A), 31, Supplement, 53
Lin J., Forbes T. G., Démoulin P., 1998, ApJ, 504, 1006
Lin J., Forbes T. G., Isenberg P. A., 2001, J. Geophys. Res., 106, 25053
Low B. C., Hundhausen J. R., 1995, ApJ, 443, 818